2011 IEEE/RSJ International Conference on
Intelligent Robots and Systems
September 25-30, 2011. San Francisco, CA, USA

A MRI-based Integrated Platform for the Navigation of Micro-devices and Microrobots

Manuel Vonthron, *Student Member, IEEE,* Viviane Lalande, *Student Member, IEEE,*
Gaël Bringout, *Student Member, IEEE,* Charles Tremblay and Sylvain Martel, *Senior Member, IEEE*

Abstract— **Magnetic Resonance Navigation (MRN) aims at navigating artificial or synthetic untethered micro-devices and microrobots using an upgraded clinical Magnetic Resonance Imaging (MRI) system. For larger MRI-based navigated entities, past experiments proved that software-based upgrades only were sufficient. But for microrobots with an overall diameter of only a few tens of micrometers for travelling in narrower blood vessels, hardware upgrades need to be added to the MR scanner, resulting in a MRN system capable of generating 3D magnetic propulsion gradients on the microrobots well above the ones that could be generated by a clinical MRI scanner relying on software-upgrades only. But with the variety of models of clinical scanners coped with many versions of related operating software dedicated to MR imaging, implementing such upgrades that could operate with these scanners becomes a real challenge. As such, a new MRN platform architecture independent of the types of MR scanners is proposed and preliminary experimental data validating the potential of such microrobotic navigation system architecture integrated with a commercially available scanner are reported. The expected steering capabilities of the platform were evaluated initially using a special probe in the form of a magnetic catheter mimicking an anisotropic microrobot. Such special probe also allowed for easier recordings of the gradient steering force that would be induced on such microrobot while validating the technique for catheter steering which is also an important aspect since catheterization is often used for releasing the microrobots in larger arteries. Similarly, MR tracking of the same microrobot was also validated with the new system, confirming that tracking feedback data can be gathered in order to perform closed-loop navigation control.**

I. Introduction

THE use of microrobots in minimally invasive medicine is becoming a trend in robotics research and different approaches have been investigated [1]. A review of these approaches suggests that magnetism is a predominant choice for moving such microscale robots. Therefore, it is not surprising that Magnetic Resonance Imaging (MRI) has not only been considered as a medical imaging modality for operations in the human body, but also for magnetic actuation purpose. Indeed, combining such magnetic actuation with a proper imaging modality allowing for the tracking of microrobots in the body opens the possibility for closed-loop servo control along pre-planned trajectories. But the implementation of such powerful concept for medical microrobots navigating in the vascular network is not a trivial task.

Indeed, ideally, the software and hardware upgrades needed to perform the navigation of microrobots must be implemented in a manner to be as independent as possible from the MR scanner being used while maintaining real-time requirements for adequate closed-loop navigation in the vascular network.

This is a major shift from the system's implementation that was initially used for a first *in vivo* proof of concept where a 1.5mm sphere was successfully navigated in the carotid artery of a living swine [2]. For this experiment, a software-only upgrade for Magnetic Resonance Navigation (MRN) was implemented within the MRI software platform and as such, the MRN upgrade was highly dependent not only on the model of MR scanner but also on the version of its software dedicated to imaging.

In the following sections, the three main components of the new MRN platform architecture for supporting *in vivo* tracking, actuation, and control are described and validated experimentally.

II. Theory of Operations

MRN-based medical interventions rely on four main functions that have been implemented in the software and hardware upgrades of this proposed interventional microrobotic platform. These are the path planning, steering of the microrobots, localization or tracking of the navigated entities, and navigational control along the pre-planned trajectory in the vascular network. They are described in the following sub-sections.

A. Path Planning

Because of the complexity of the system, the technical constraints, and the physics associated with such types of operations, path planning is a critical part of MRN interventions. First, a high resolution MR image of the Region of Interest (ROI) is taken using a regular MRI angiographic sequence. The scan image is filtered as needed to highlight the vessel network of the patient. A path consisting of several "waypoints" along the vessels is defined, starting from an injection point of the microrobot to the actual target, e.g. a chemoembolization site for the release of a therapeutic agent in cancer therapy. This path planning would then determine the roadmap or trajectory to be followed by a microrobot or an aggregation of microrobots. Such trajectory is also the reference path used by the real-time closed-loop controller dedicated to navigation. The absolute positioning developed and described in [3] detects with a high precision

This project is supported in part by the Canada Research Chair (CRC) in Micro/Nanosystem Development, Fabrication and Validation and grants from the National Sciences and Engineering Research Council of Canada (NSERC), the Province of Québec, and the Canada Foundation for Innovation (CFI).
Corresponding author: Sylvain Martel, NanoRobotics Laboratory, École Polytechnique de Montréal, 2500 chemin de Polytechnique, Montréal (QC), Canada, H3T 1J4. (E-mail: sylvain.martel@polymtl.ca)

Figure 1: Path planning: definition of the reference trajectory (roadmap).

the location of the microrobot and apply a registration algorithm on the roadmap. Presently, the roadmap or trajectory is defined and plotted in the custom software application depicted in Fig.1.

B. Steering

A magnetic force $\vec{F}_{mag}$ is induced in the soft magnetic core of the microrobot and is expressed as

$$\vec{F}_{mag} = RV_m \cdot \left(\vec{M} \cdot \vec{\nabla}\right)\vec{B} \quad (1)$$

where V_m is the volume of the ferromagnetic core or the microrobot if its volume is entirely magnetic (m^3), $\vec{M}$ is its magnetization (A/m) which is typically at full saturation when placed in the bore of a clinical MRI scanner, $\vec{\nabla B}$ is the magnetic gradient field applied, and R is defined here as the duty cycle, i.e. the time when magnetic gradients used for propulsion or steering are applied within a cycle. Indeed, previous experiments with a clinical MRI system [4] were based on modified pulse sequences to generate a magnetic gradient used as a mean of propulsion rather than imaging. The new actuation hardware is conceived with this goal in mind, allowing stronger force and longer application duration. In all cases, a combination of three gradient coil sets, one for each direction of the space, is used.

C. Localization

The microrobot needs to be accurately tracked within real-time constraints to enable closed-loop navigation control. The dynamic positioning is achieved through a technique specially developed for such an application and which is known as Magnetic Signature by Selective Excitation Tracking (MS-SET) [5].

This positioning method relies on magnetic susceptibility artifacts caused by the ferromagnetic core. Instead of correcting for the distortion in the image, this physical difference with the rest of the volume to capture the magnetic signature of the device or robot is taken into account. First, a RF pulse tuned to the frequency of selected equipotential curves caused by the ferromagnetic core is emitted. The RF signal emitted by the targeted protons with a regular readout gradient is gathered at a selected equipotential curve frequency. This results in three orthogonal acquisitions from which a 3D localization is obtained. The first set of projections is used as the basis of the correlation function for further acquisitions. Thus, 3D relative coordinates can be obtained with the acquisition of only three *k-space* lines (usually 256 lines), resulting in a considerable gain in speed compared to standard imaging acquisition and also in terms of image processing. This technique allows a sub-millimeter precision with a frequency acquisition up to 30Hz [6].

D. Control

A 3D PID controller has been successfully designed and implemented inside the MRI's framework to compute the deviation of the device from the ideal motion from tracking information gathered in real-time. From such feedback data, the controller was then able to compute and to generate the required propulsion gradient values for corrective actions in order to maintain the micro-device or microrobot along the planned trajectory. Although a PID controller proved to be appropriate for the first proof-of-concepts, more advanced control algorithms based on predictions and taking into consideration not only physiological conditions but also technological constraints within the MRN system would most likely lead to better performance.

III. Towards an Upgraded Platform

Although all the procedures listed in the previous section have been validated experimentally [7], a clinical MRI system usually provides gradient magnitude from only 10 to 60 mT/m [8]. In some previous experiments, the gradient magnetic field induced a force on a relatively large ferromagnetic object (e.g. a 1.5mm bead). However, the magnetic force (see Eq. 1) produced by such gradients depended on the size of the magnetic core and as experimented in [7] and also mentioned in [9], such gradient amplitudes cannot steer properly a sub-millimeter device or robot in real physiological conditions. Furthermore, since the force is proportional to the cube of the spherical device or robot diameter (Eq. 1), the need for more gradient amplitudes becomes quickly necessary when the size of the microrobot must be decreased to travel in narrower blood vessels. Moreover, as described in [10], although the effective volume (Eq. 1) of magnetic material can be increased with an aggregation of smaller microrobots, the imaging gradient coils and their associated power-supply cannot experience a duty cycle typically higher than 50% at full amplitude. On a Siemens Sonata MRI system for instance, this fact leads to effective gradient amplitudes in the order of only 20mT/m (versus 40mT/m). Therefore, higher magnetic gradient amplitudes estimated at several hundreds mT/m [10], i.e. well beyond the capability of regular scanners, are required. On the software point of view, MRI systems come in various models and configurations with operating software systems that are not only different but that are modified (upgraded) by the manufacturer on a regular basis. These changes make the

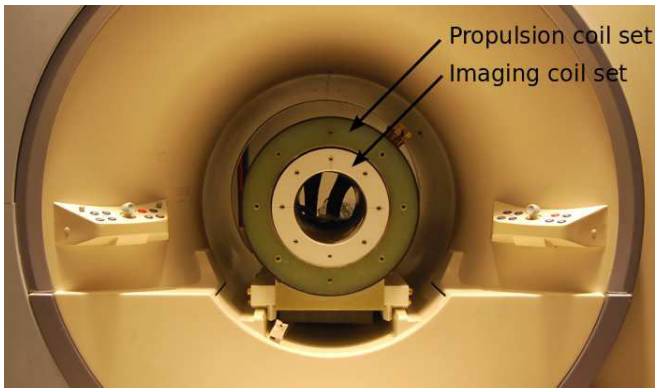

Figure 2: Magnetic gradient coil sets inside the bore of a 1.5T Siemens Sonata MRI system - The outer cylinder is responsible of high amplitude and duty cycle gradients for propulsion. The inner cylinder provides high linearity and responsiveness gradients for imaging purpose.

tight integration of additional software functionalities dedicated to MRN with commercial MRI software very difficult and challenging since modifications will always be necessary to deal with these changes initiated by the manufacturers. MRI systems are also very complex equipments dedicated to medical uses where safety is crucial. This also explains in part the fact that the platform is "locked" and few opportunities are given to allow usage of a clinical system for research purpose. A strong emphasis is therefore given on the new system that uses standard and open computing components, software and protocols.

The new platform we present here offers gradient coils of 450 mT/m capabilities in the three directions of space. We designed a whole hardware and software platform able to fulfill MRN for smaller microrobots while not requiring any change to a regular clinical MRI apparatus. In other words, we propose a manufacturer-independent and model independent solution that maintains the existing MRI equipment unchanged.

IV. Hardware components

To achieve the goal of steering catheters, microparticles and other micro-devices including microrobots, two sets of coils are added as a complement of the existing equipment being in our case a 1.5T Siemens Sonata clinical MRI system. No hardware or software modification was done on the hosting system allowing MR imaging functionality and other functions related to MRI to be used.

A. Propulsion System

The new actuation (propulsion and steering) system (Fig. 2) is made of a 400mm outer diameter cylinder embedding three pairs of magnetic gradient coils. A pair of longitudinal coils generates the *z*-axis (along the longitudinal of the MRI bore) gradient up to 510mT/m. Two pairs of transversal coils provide *x* and *y*-axis gradients, up to 460mT/m. A dedicated power supply and cooling system allow for operations with a 100% duty cycle at the cost of a lower slew rate that translates to a minimum rise time of the coils and amplifier of 20ms. Depending on the interventions, such longer rise time is typically acceptable for propulsion but cannot allow imaging with the same equipment.

Indeed, the propulsion coil set has been designed to maximize the magnetic force on the microrobots but by doing so, it could not be designed to be used for medical imaging since its ramp up time and gradient uniformity are below the specifications required for high quality medical imaging.

B. Imaging and Tracking System

In our platform, the imaging and tracking coil set (Fig.2) reproduces the imaging capability of the MRI system, yet with higher imaging gradient amplitudes. The main characteristics of the coils is the ability to have very small rise time, down to 100µs, providing MRI quality images. Imaging pulse sequences usually do not need gradient amplitude higher than a few mT/m. The use of stronger gradient amplitude allows shortening the duration of the pulse and increasing the tracking rate.

V. Software architecture

The use of microrobots in minimally invasive surgery requires that the system is built upon highly reliable pieces of software. The architecture involves synchronization and communication between heterogeneous equipments. We choose to run a central controller computer running a hard real-time operating system (RTOS).

A. Xenomai

Among the large number of available operating systems, only a few of them are able to guarantee hard real-time performance. Examples of RTOS include known commercial systems such as VxWorks (WindRiver) or QNX (Research In Motion). Real-time capabilities also have been added to the Linux kernel through projects such as RTAI or the `PREEMPT_RT` patch and provide comparable if not better performances [11]. We use the Xenomai framework, an RTAI's derivative, which provides a double kernel solution to handle hard real-time requirements. Our experience with Xenomai showed that it provides many facilities such as good hardware support, message passing framework, real-time interface drivers suitable for our platform. Furthermore, the framework allowed us to develop hard real-time applications in both kernel-space and user-space. Xenomai comes with the Analogy framework that we used to interface our controlling station with non-serial and non-network communication link such as TTL lines for synchronization or analog sampling for enhancing predictive navigation control of the microrobots by gathering more physiological data that may include electrocardiograph (ECG) and other physiological-related sensory information. The physical interface was achieved with a PCI acquisition card (PCI-6036E, National Instruments, USA) programmed through the `ni_pcimia` driver of the Analogy framework.

B. Synchronization

The main computer manages heterogeneous equipment and runs the low level controller. The three major components of the system run in a time-multiplexed fashion (Fig. 3). Once the tracking pulse sequence is completed, the resulting raw RF data are sent to the controller which will

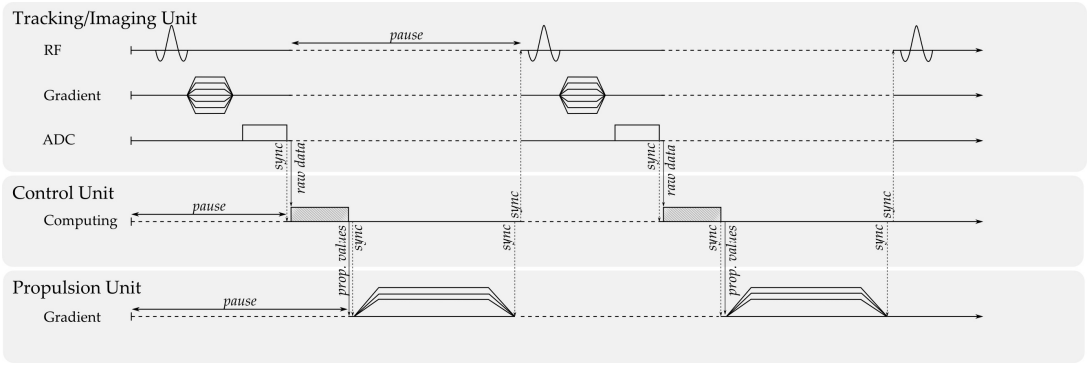

Figure 3: Sequence of events – Upper part depicts the MRI-based tracking sequence with a tuned RF pulse. Bottom part shows the propulsion unit driven by commands computed by the control unit (middle part).Imaging and propulsion events are mutually exclusive: precise synchronization and control is achieved by the main controller.

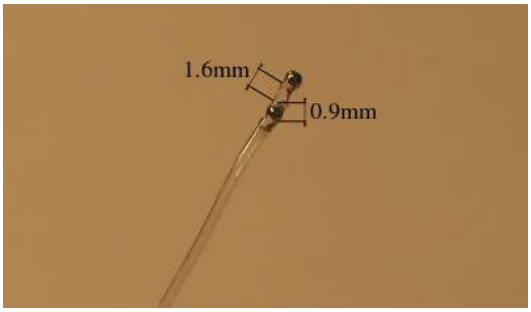

Figure 4: Distal tip of the catheter provided with two ⌀0.9mm chrome steel beads.

then compute the correlation, deduce the movement of the targeted microrobot and generate the appropriate propulsion sequences. Such tracking and propulsion components represent the environment of the real-time scheduling role played by the controller.

VI. Microrobots and Catheters

Although the strong homogeneous magnetic field (e.g. 1.5T in our case) of the MR scanner will saturate the soft ferro-magnetic material of the microrobot, leading to maximum propulsive or steering force, the same field will also align such microrobot along the longitudinal axis of the MRI bore, also known as the z-axis. Therefore, previous versions of microrobots designed to maneuver inside a MRI bore were rounded in shape such that the drag coefficient would be the same in all directions while the orientation of the microrobot would remain constant during travel. Although, effort could be put forward to optimize the microrobot shape to reduce fluid drag relative to magnetic forces, such effort would not yield a significant improvement since a simple spherical microrobot would only have approximately 10% higher fluid drag compared to the one with an optimal shape [12].

Nonetheless, although an aggregation of smaller microrobots can yield higher propulsive force through interactive coupling due to dipole-dipole interactions between the microrobots, a similar approach can be investigated and potentially applied for the implementation of an anisotropic microrobot instead of spherical versions mentioned earlier.

One approach for the implementation of an anisotropic microrobot would be the integration of two mechanically coupled distant magnetic spheres within a longitudinal body, e.g. a cylinder. This design would add to the effective volume of magnetic material for an increase in the magnetic force being induced (see Eq. 1). But such implementation to be effective in the vasculature would be complicated by the fact that the high magnetic field of the MR scanner would induce a constant torque on the spheres that would have to be taken into account.

To investigate the basic principle of this approach, a special tip has been designed at the end of a catheter as shown in Fig. 3. This experimental method yielded easier measurement gatherings while demonstrating the possibility of steering a catheter that could be more easily positioned in specific locations suitable for the release of the microrobots.

VII. Preliminary Experiments

A. Propulsion and Steering Measurements

A 2.5Fr catheter ("FasTracker 018", Boston Scientific, USA) of a 1.2×10^{-6} N.m^2 bending stiffness was clamped at 42mm from its distal tip. The tip of the catheter was composed of two ferro-magnetic chrome steel beads (Salemball, USA) spaced one from another with a hand-made PMMA spacer 1.6mm long. The clamp and catheter were placed in a water bath to reduce friction. Each bead had 0.9mm diameter with a 1248 kA/m saturation magnetization. During the experiments, the gradient generated varies from -400mT/m and +400mT/m by steps of 50mT/m. The displacement of the catheter relatively to its natural position when no gradient was applied was measured at each step with a MRI compatible camera. The setup was placed between a pair of Maxwell coils (Fig 5(a)) and in the bore of a 1.5T Siemens Sonata MRI system so that the beads could reach their saturation magnetization. The Maxwell coils were powered in order to produce a gradient along the z axis of the MRI system. The same setup was then placed at the center of the propulsion coil cylinder inside the bore of the MRI system. This is depicted on Fig. 6(a). The free end of the catheter was placed in the homogeneity sphere of the coils set perpendicularly to the z axis.

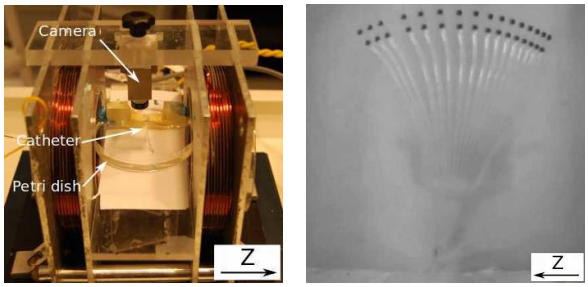

(a) (b)

Figure 3: Comparison experiment: (a) shows the experimental setup; (b) is a superimposed picture of the deflections obtained by varying the gradient amplitude by 50mT/m increments from -400mT/m to +400mT/m.

Figure 5(b) and 6(b) show superimposed photographs of the deflections of the catheter inside the Maxwell coils and the propulsion coil set respectively. Each photograph represents a 50mT/m increment. Maximum amplitude and minimum amplitude correspond to our top values of 400 and -400mT/m. The comparison of the two pictures shows a highly similar behavior of the catheter regardless of the coil used. Figure 7 represents the displacement amplitude of the catheter relatively to the gradient amplitude applied for both systems. They both experience an increasing displacement with the gradient field as well as a displacement difference between the two sides of the experiment. This phenomenon is explained by the existence of an unwanted preferential magnetization direction of the bead possibly due to the grain anisotropy inside the material. The two curves show a good correlation that validates the ability of the new coils to generate a magnetic force with the expected amplitude.

B. Tracking Measurements

As the complete tracking set was not yet completely assembled, the tracking method was initially validated with a clinical MRI system on the same type of catheter tip used in the propulsion and steering experiment. These tracking measurements were achieved independently from the propulsion test.

A one-bead tip catheter representing a potential microrobot was manually moved inside a glass phantom mimicking a blood vessel in order to track the bead in *in vitro* conditions. The phantom depicted on Fig. 8 was placed on a plastic stand used to lift it at the center of the homogeneous MRI system's zone. The phantom had a 2.8mm internal diameter with a length of 135mm. The setup was immersed into a water filled spherical aquarium to make sure that the catheter tip was surrounded with a large quantity of hydrogen protons for tracking requirements. The catheter was then manually moved inside the glass phantom from one end to the other.

A tracking MRI sequence was run during the actuation of the catheter. The sequence was tuned to best detect the displacement of the tip's bead by adjusting the excitation and acquisition frequency. The appropriate frequency offset was found by trials and errors. As soon as a displacement was computed, its coordinates were recorded in a text file. We performed a registration step on the collected data from the tracking program to match the coordinate origin. The points (X, Z) were then loaded as a "fiducial list" in the

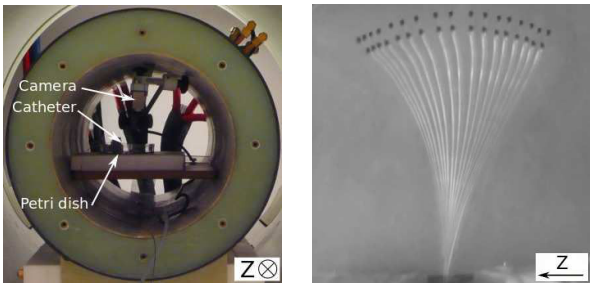

(a) (b)

Figure 6: Transposition of the experimental setup for the new propulsion system: (a) shows the setup inside the new gradient coil set; (b) represents the superimposed pictures of the deflections obtained by varying the gradient amplitude by 50mT/m increments from -400mT/m along the *z* axis.

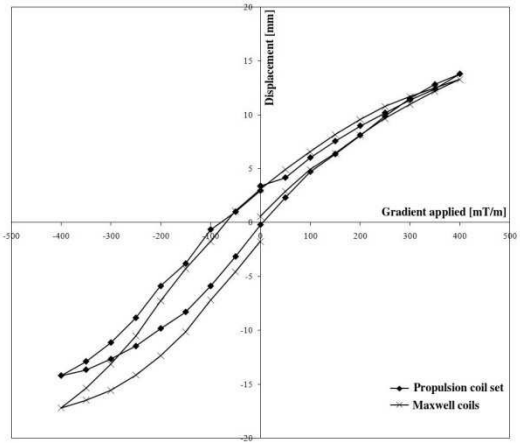

Figure 7: Graphs showing the displacement of the catheter versus the gradient amplitude inside the propulsion coil set and the Maxwell coils.

medical imaging visualization and computing software 3DSlicer.

Figure 9 shows the evolution of the tracked points coordinates versus time. X and Z axis are plotted. The positions of the catheter are also depicted in Fig. 10 as a view similar to what we are proposing to offer to the medical team during an operation. The image taken at the beginning of the procedure (path planning) is used as a background image to the point visualization. In this experiment, we ran a regular HASTE imaging sequence on the model. The combination of the image and the tracked points shows that the expected trajectory is tracked as expected. Variations on the *x*-axis while the catheter is moved forward can be explained by the movement of the 0.9mm diameter tip inside the 2.9mm diameter tube and/or the tracking errors of the test. Maximum amplitude of this variation is up to 3.2mm. Considering the inner diameter of the model, this remains an acceptable precision to enable a closed-loop control on this basis for not only catheters but also microrobots.

VIII. DISCUSSION AND CONCLUSION

The propulsion abilities of our new set of coils have been tested and they successfully provided the magnetic force needed to bend a catheter as expected while providing insights about the possibility of steering much smaller microrobots. The tracking sequence has successfully been

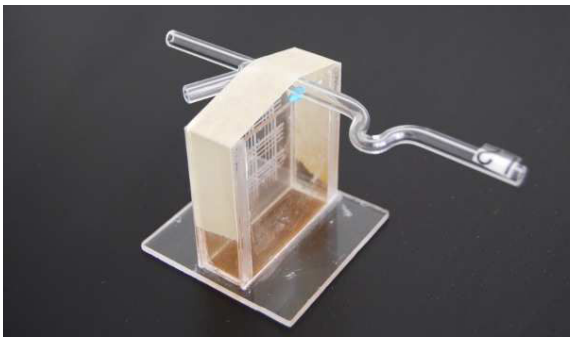

Figure 8: Glass phantom mimicking curve and bifurcation of a blood vessel.

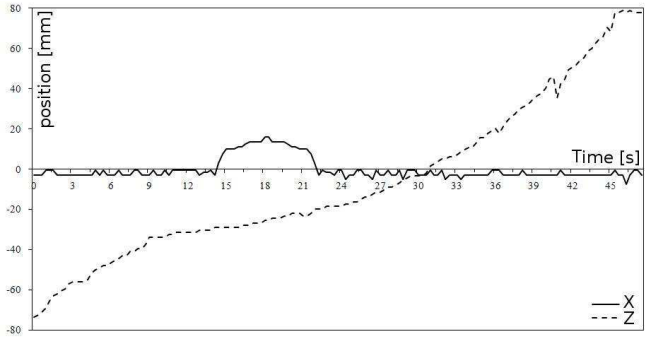

Figure 9: Evolution of (Z, X) positions from tracking method while moving the catheter into the phantom.

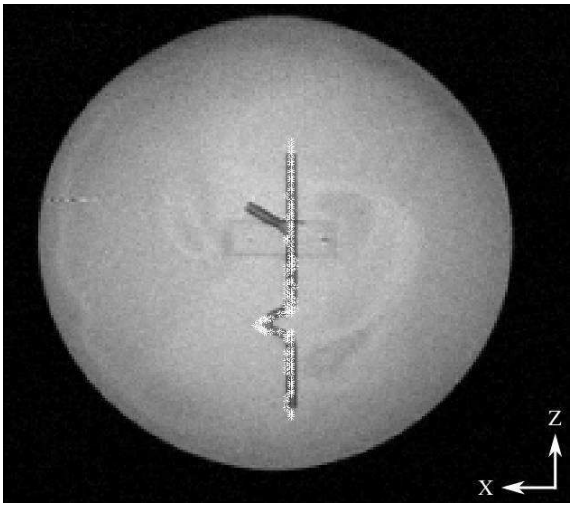

Figure 10: Result of the tracking in the glass phantom in a spherical aquarium. The dots represent the catheter tracked points as viewed in the fiducials module of 3DSlicer (medical imaging software). Axis added.

achieved on a catheter mimicking the signal that could be generated from a microrobot. Many tasks still remain to complete a whole new platform and each component has to be tested and validated.

Thus, future work will focus on the transfer of the tracking techniques developed on MRI system on our new set of imaging coils. The synchronized activation of the propulsion and tracking elements through the main controller will be thoroughly tested. Validation of these techniques will allow starting the making of a human scale gradient system, whereas a rabbit-sized system has been presented, considering the high cost and complexity of such an equipment.

Further applications of this integrated system will also drive smaller microrobots which are much more demanding for real time hardware/software implementations and rise time for the propulsive coils. Examples of potential applications include but are not limited to the treatment of cancer by bringing drugs closer to the tumor rather than releasing it systematically into the bloodstream. The potential advantages of such platform capable of navigating microrobots are important since chemotherapeutic drugs are toxic even for healthy cells, thus causing massive side effects.

ACKNOWLEDGMENT

The authors wish to acknowledge the support of the Nanorobotic Laboratory of Ecole Polytechnique de Montréal (EPM) and particularly Ouajdi Felfoul from the same lab. Previous teams of the Nanorobotic Laboratory that participated in projects related to this platform are also acknowledged as this work takes its foundation on their past breakthroughs and experimental validations.

REFERENCES

[1] B. J. Nelson, I. K. Kaliakatsos, and J. J. Abbott, "Microrobots for minimally invasive medicine," *Annual Review of Biomedical Engineering*, vol. 12, pp. 55–85, June 2010.

[2] S. Martel, J.-B. Mathieu, O. Felfoul, A. Chanu, E. Aboussouan, P. Pouponneau, G. Beaudoin, G. Soulez, and M. Mankiewicz, "Automatic navigation of an untethred device in the artery of a living animal using a conventional clinical magnetic resonance imaging system," *Applied Physics Letters*, vol. 90, p. 114105, 2007.

[3] E. Aboussouan and S. Martel, "High precision absolute positioning of medical instruments in MRI systems," in *Proceedings of 28th Annual International Conference of the IEEE in Engineering in Medicine and Biology Society EMBS,* August, 2006, pp. 743–746.

[4] S. Martel, J. Mathieu, O. Felfoul, A. Chanu, E. Aboussouan, S. Tamaz, P. Pouponneau, G. Beaudoin, G. Soulez, and M. Mankiewicz, "A computer-assisted protocol for endovascular target interventions using a clinical MRI system for controlling untethered microdevices and future nanorobots," *Computer Aided Surgery*, vol. 13, no. 6, pp. 340– 352, 2008.

[5] O. Felfoul, J. Mathieu, G. Beaudoin, and S. Martel, "In vivo MR-tracking based on magnetic signature selective excitation," *IEEE Transactions on Medical Imaging*, vol. 27, no. 1, pp. 28–35, 2008.

[6] O. Felfoul, E. Aboussouan, A. Chanu, and S. Martel, "Real-time positioning and tracking technique for endovascular untethered micro-robots propelled by MRI gradients," *In Proc. of the IEEE Int. Conf. on Robotics and Automation*, 2009.

[7] J. Mathieu and S. Martel, "In vivo validation of a propulsion method for untethered medical microrobots using a clinical magnetic resonance imaging system," in *Proceedings of the IEEE/RSJ Int. Conf. on Intelligent Robots and Systems (IROS)*, San Diego, CA, 2007.

[8] C. Westbrook, C. Roth, and J. Talbot, *MRI in Practice*. Wiley-Blackwell, 2005.

[9] K. Belharet, D. Folio, and A. Ferreira, "MRI-based microrobotic system for the propulsion and navigation of ferromagnetic microcap-sules," *Minimally Invasive Therapy & Allied Technologies*, vol. 19, no. 3, pp. 157–169, 2010.

[10] J. Mathieu and S. Martel, "Steering of aggregating magnetic microparticles using propulsion gradients coils in an MRI Scanner," *Magnetic Resonance in Medicine*, vol. 63, no. 5, pp. 1336–1345, 2010.

[11] A. Barbalace, A. Luchetta, G. Manduchi, M. Moro, A. Soppelsa, and C. Taliercio, "Performance comparison of VxWorks, Linux, RTAI and Xenomai in a hard real-time application," *IEEE Trans. Nucl. Sci.*, vol.53, pp. 1015-1021, Jun. 2008.

[12] F.A. Hinojosa and S. Martel, "Suggested shapes for a first generation endovascular untethered microdevice prototype," *Proc. IEEE Int. Conf. Eng. Med. Biol. Soc.*, Shanguai, China, pp. 1286-1288, Sept. 1-4, 2005.